

Analysis of phase shifter length for forward biased silicon-on-insulator (SOI) optical modulator

A. R. HANIM, P. S. MENON*, S. SHAARI, H. HAZURA, B. MARDIANA

Photonics Technology Laboratory (PTL), Institute of Micro Engineering and Nanoelectronics (IMEN), Universiti Kebangsaan Malaysia, 43600 UKM, Bangi, Selangor, Malaysia

This paper investigates the performance of a three-dimensional virtual model of a Silicon-on-Insulator (SOI) optical phase modulator using an industrial-based numerical simulator. The 3 dB bandwidth of the device was analyzed by varying the phase shifter length to 6, 12 and 18 μm . Then, the effect of varying the phase shifter length to different concentration of boron (p+ doped well) and phosphorus (n+ doped well) was observed. It can be deduced that with appropriate applied voltage selection, the device performs the best at 6 μm phase shifter length and at higher concentration of the doped wells. The best performance of the device is at 1V, with 3 dB bandwidth of 1.4THz.

(Received December 6, 2012; accepted April 11, 2013)

Keywords: Phase shifter length, SOI current injection modulator, 3 dB bandwidth

1. Introduction

The need for smaller size of CMOS devices has spurred growing interest in replacing conventional electrical interconnects to optical interconnects. Using photons in place of electrons in data transmission can double the bandwidth, decrease the power usage, increase the speed of the device and laying a possibility of a more complex device design. However, classical materials for optical interconnects such as indium phosphide, lithium niobate, gallium arsenide are expensive and integration of optical and electrical devices on the same substrate are impossible. Therefore, development of optical devices on silicon substrates particularly the Silicon-On-Insulator (SOI) is attractive in order to allow the possibility of manufacturing optoelectronics devices. The mature and low-cost silicon complementary metal-oxide-semiconductor (CMOS) technology is an advantage in order to fabricate monolithic micro-photonics circuits besides its high refractive index contrast [1,2].

The optical modulator, which writes data onto the optical carrier, is one of the crucial elements in photonic circuits. Demonstrations of optical modulation in silicon utilizing the plasma dispersion effect have been done by several groups of researchers and is in favor compared to other types of modulation due to its high performance, fabrication simplicity and CMOS compatibility [3-5]. The plasma dispersion effects allow changes in the refractive index by changes in the electrons and holes concentration. Various research have been undertaken utilizing the three types of plasma dispersion effects which are the accumulation, injection and depletion of holes and electrons concentration [6-8].

Apart from optical communication systems, phase shifters can also be used as sensors where change in the cladding refractive index occurs when the rib waveguide is exposed to different analytes. Optical sensors can either be in the form of optical waveguide devices or tapered

optical-fiber-based sensors [9]. However, this work reports on the analysis of optical modulators applicable to optical communication systems.

Different structures of p-n junction as a phase shifter in an optical modulator exhibited a 3 dB bandwidth of 14GHz [10], 6MHz [11], 26GHz [12] and 30 GHz [13], to quote a few. Studies on the effect of varying the phase shifter length for silicon modulator based on carrier depletion effect have been demonstrated [3,10,13]. A similar structure from our previous work was adopted and modified in order to develop a 3D model of an optical modulator [14]. To the best of our knowledge, a comparison in 3 dB bandwidth for different phase shifter length with different n+ and p+ concentration for SOI optical phase modulator based on current injection effect in a 3D simulator has only been performed in this work. This approach saves time and cost prior to fabrication and implementation in optical communication systems.

2. Methodology

The modeling was performed using TonyPlot3D software. It is a powerful graphics tool, capable of displaying 3D TCAD data generated by Silvaco TCAD process or device simulators and Silvaco's 3D parasitic products. It provides visualization and graphic features such as zoom, pan, views and different drawing modes. TonyPlot3D provides a user-friendly environment to view 3D structures in various TCAD specific display modes such as regions, contours, rays, isosurfaces and vectors [15].

Fig. 1 shows the cross section of the optical phase modulator. The rib width and height is 0.5 μm and 0.55 μm respectively. The values of the rib width and height were selected as such to maintain a single mode condition [16]. At three phase shifter lengths, which were 6, 12 and 18 μm ,

the concentrations of boron (p+) and phosphorus (n+) were varied as in Table 1.

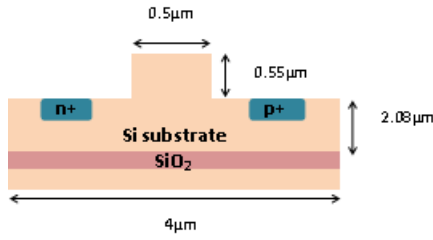


Fig. 1. Cross section of the optical modulator.

Table 1. Parameters for optical modulator design.

Parameter	Value 1	Value 2
p+, boron concentration (cm ⁻³)	5e17	5e19
n+, phosphorus concentration (cm ⁻³)	5e7	5e9

The switching characteristics of the phase modulator were evaluated using the transient modeling solution. The rise time t_r is defined as the time required for the anode current to change from 10% to 90% of the maximum value. Likewise, the fall time t_f is defined as the time required for the anode current to change from 90% to 10% of the maximum value. The 3 dB bandwidth is defined as $BW_{3dB} = 0.35/t_{MAX}$ where t_{MAX} is the longer of the fall time and the rise time [17].

3. Results

The usage of the TonyPlot 3D software allows numerical evaluation performed according to the device's length. Fig. 2 shows the three dimensional view of the phase modulator with 12 µm phase shifter length. The p+ and n+ wells are beneath the aluminium layers of anode and cathode on each side of the waveguide.

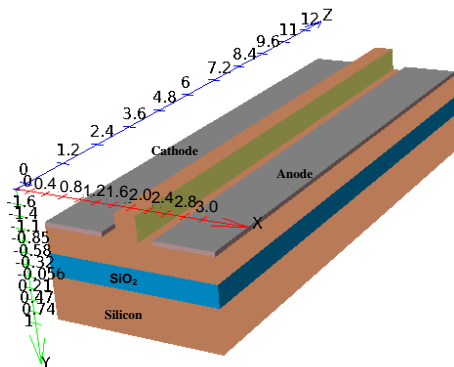


Fig. 2. Three dimensional view of the optical phase modulator.

4. Phase shifter length variations

Firstly, the performance of the device was analyzed by varying the phase shifter length at two values of p+ and n+ concentrations. Fig. 3 depicts the 3 dB bandwidth of the device at concentrations p+ and n+ of 5e19cm⁻³ and 5e9cm⁻³ respectively. As can be seen, from 0.8V to 0.9V, the 3 dB bandwidth of device with shorter length performs better than the longer ones with small differences of bandwidths for each phase shifter length. However, for voltage greater than 0.9V, the trend changes. For example, at approximately 0.935V, the bandwidth of 6µm phase shifter length experiences a sudden decrease. At this point, longer device performs better. Beyond this point, device with 6µm phase shifter length gains the highest bandwidth at 1V.

Fig. 4 shows the performance of the device with different phase shifter lengths at concentrations of 5e17cm⁻³ and 5e7cm⁻³ for p+ and n+ respectively. It can be seen that the device with 18 um phase shifter length, the bandwidths for 0.8 to 1.0V are almost static. At 0.85V, the three devices with different lengths gain almost equivalent 3 dB bandwidths.

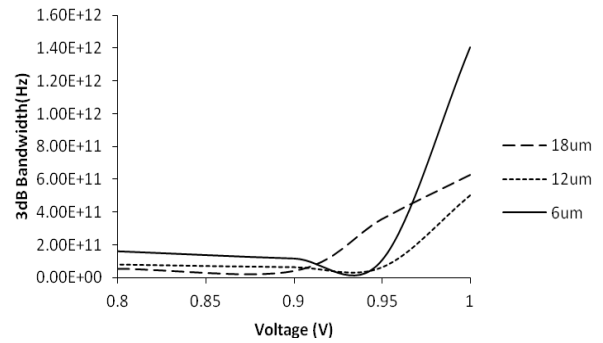


Fig. 3. 3 dB bandwidth for concentration p+=5e19cm⁻³, n+=5e9cm⁻³.

Meanwhile, at 0.95V, device with phase shifter length of 6 and 12µm decreases before gaining higher bandwidth at 1V. At 1V, the highest bandwidth belongs to 6µm phase shifter device, followed by 12µm and 18µm phase shifter devices.

In all, the 6µm phase shifter device gains highest bandwidth in comparison with longer devices, attaining highest 3 dB bandwidth at 1V. Shorter phase shifter length allows a more concentrated active area thereby more interactions among the holes and electrons occur resulting in a better performance device with appropriate selection of applied voltage.

5. Concentration variations

The analysis of the modulator resumes by varying the p+ and n+ concentrations for different phase shifter lengths as depicted in Fig. 5, Fig. 6 and Fig. 7.

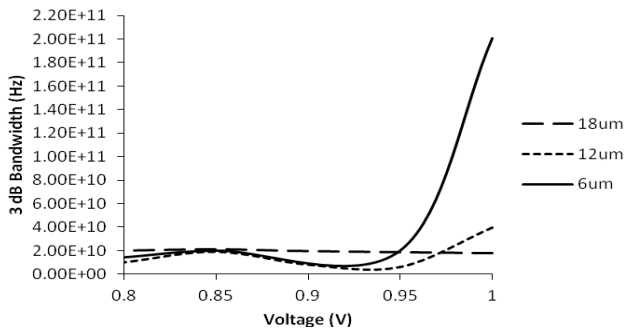


Fig. 4. 3 dB bandwidth for concentration $p+=5e17cm^{-3}$, $n+=5e7cm^{-3}$.

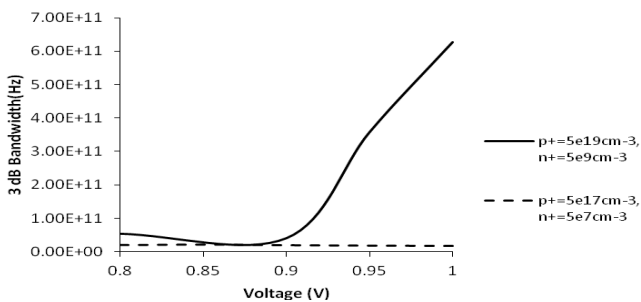


Fig. 5. 3 dB bandwidth at phase shifter length of 18 μm .

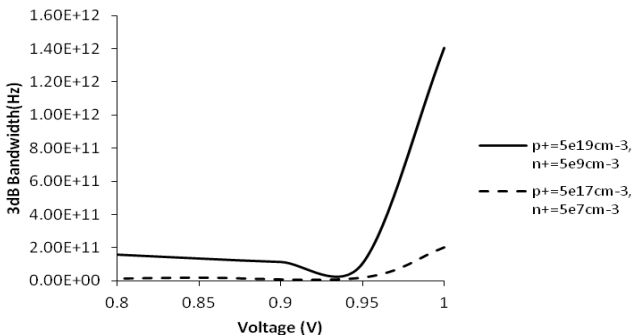


Fig. 7. 3 dB bandwidth at phase shifter length of 6 μm .

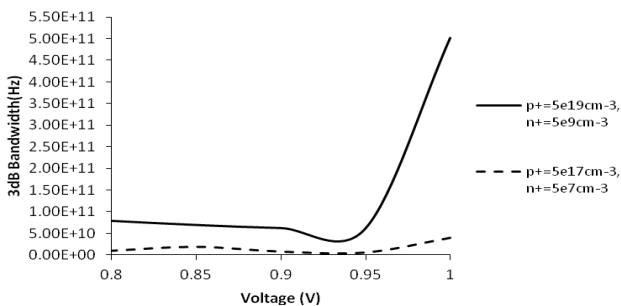


Fig. 6. 3 dB bandwidth at phase shifter length of 12 μm .

From these graphs, it can be deduced that devices with higher $p+$ and $n+$ concentrations gain higher 3 dB bandwidth regardless of phase shifter length. For devices

with $p+$ and $n+$ concentrations of $5e19 cm^{-3}$ and $5e9 cm^{-3}$, the bandwidth drops before a sudden increase at 1V. Meanwhile, 6 μm phase shifter device gains highest bandwidth with 1.4THz at 1V. Higher concentrations of $p+$ and $n+$ introduce more electrons and holes to the active region and thus more interactions among the electrons and holes.

6. Conclusion

An optical phase modulator on SOI has been implemented by 3D numerical modeling. The performance of the device was analyzed by varying the phase shifter length of the device. Then, the effect of varying the phase shifter length to different concentrations was analyzed. It can be deduced that with appropriate voltage selection, the device performs the best at 6 μm phase shifter length and at higher concentration of $p+$ and $n+$. The best performance of the device is at 1V, with 3 dB bandwidth of 1.4THz. Usage of numerical evaluation prior to actual device fabrication reduces device fabrication cost and time as well as provides an insight into the physics of the device which may not be executable in the actual fabricated device.

Acknowledgement

The authors would like to thank Universiti Teknikal Malaysia Melaka (UTeM) for the support and Institute of Microengineering and Nanoelectronics, Universiti Kebangsaan Malaysia for funding this research under grant Industri-2012-017.

References

- [1] G. T. Reed, A. P. Knights, Silicon photonics. Wiley (2008).
- [2] M. Ibrahim, N. Mohd Kassim, A. Mohammad, Optoelectron. Adv. Mater. Rapid Commun. **3**, 917 (2009).
- [3] D. J. Thomson, F. Y. Gardes, Y. Hu, G. Mashanovich, M. Fournier, P. Grosse, J-M. Fedeli, G. T. Reed, Optics Express **19**, 11507 (2011).
- [4] Ning Ning Feng, Shirong Liao, Dazeng Feng, Po Dong, Dawei Zheng, Hong Liang, Roshanak Shafiiha, Guoliang Li, John E. Cunningham, Ashok V. Krishnamoorthy, Mehdi Asghari, Optics Express **18**, 7994 (2010).
- [5] B. Jalali, S. Fathpour, Journal of Lightwave Technology **24**, 4600 (2006).
- [6] L. Liao A. Liu, J. Basak, H. Nguyen, M. Paniccia, D. Rubin, Y. Chetrit, R. Cohen, N. Izhaky, Electron. Lett. **43**, 1196 (2007).
- [7] A. R. Hanim, B. Mardiana, H. Hazure, S. Shaari, IEEE International Conference on Photonics **1**, (2010).
- [8] F. Y. Gardes, G. T. Reed, N. G. Emerson, Optics Express **13**, (2005).
- [9] Wan Maisarah Mukhtar, P. Susthitha Menon,

- Sahbudin Shaari, *Optoelectron. Adv. Mater. - Rapid Commun.* **6**(11-12), (2012).
- [10] A. Mao, J. Liu, D. Gao Z. Zhouet, *Electronic Letters* **44**, (2008).
- [11] R. W. Chuang, M. T. Hsu, Y.C. Chang, Y. J. Lee, *IET Optoelectronics* **6**, (2012).
- [12] Steven J. Spector Cheryl M. Sorace, Michael W. Geis, Matthew E. Grein, Jung U. Yoon, Theodore M. Lyszczarz, Erich P. Ippen, Franz X. Kärtner, *IEEE Journal of Selected Topics in Quantum Electronics* **16**, (2010).
- [13] Ansheng Liu, Ling Liao, Doron Rubin, Juthika Basak, Yoel Chetrit, Hat Nguyen, Rami Cohen, Nahum Izhaky and Mario Paniccia, *Journal of Semiconductor Science and Technology* **23**, (2008).
- [14] P. S. Menon, B. Bais, J. H. I. Aimi Azri Mohd, S. Shaari, *Optoelectron. Adv. Mater. - Rapid Commun.* **6**(5-6), (2012).
- [15] *Silvaco Manual*, Silvaco Inc Santa Clara (2011).
- [16] S. P. Pogossian, L. Vescan, A. Vonsovici, *IEEE Journal of Lightwave Technology* **16**, (1998).
- [17] A. R. Hanim, B. Mardiana, H. Hazura, P. S. Menon, S. Shaari, *International Conference on Enabling Science and Nanotechnology* **1341**, (2011).

*Corresponding author: susi@eng.ukm.my